ChemComm
Chemical Communications

Accepted Manuscript

This article can be cited before page numbers have been issued, to do this please use: A. Thakur, S. Bedajna, M. Karimi and F. P. Gabbaï, *Chem. Commun.*, 2026, DOI: 10.1039/D6CC02816K.

ROYAL SOCIETY OF CHEMISTRY

rsc.li/chemcomm

ChemComm

View Article Online
DOI: 10.1039/D6CC02816K

COMMUNICATION

Macrocyclic stibine-bridged [1.1.1] and [1.1.1.1] ferrocenophanes

Arunabha Thakur,*[a] Shantabh Bedajna,[a] Mohammadjavad Karimi[a] and François P. Gabbaï *[a]

Received 00th January 20xx,
Accepted 00th January 20xx

DOI: 10.1039/x0xx00000xs

Our interest in the design of antimony-bridged ferrocenophanes has led us to revisit the reaction of 1,1′-dilithioferrocene with $PhSbCl_2$, leading to the isolation of the corresponding [1.1.1] and [1.1.1.1] ferrocenophanes, whose macrocyclic structure has been verified by X-ray diffraction. The [1.1.1] ferrocenophane has been used as a ligand for gold(I) halides, affording, in the case of the chloride derivative, a complex that exhibits carbophilic reactivity.

Phosphorus-bridged [1]ferrocenophanes[1, 2] have drawn significant attention, not only for the generation of polymers[3-9] but also as precursors for macrocycles,[10] including trimeric ones such as **I**,[10] which has been used as a tridentate ligand for transition metals.[10] Efforts directed toward heavier analogs of such systems have emerged, including in the case of arsenic[11] and antimony. Two recent publications have described the first example of such antimony-based systems.[12, 13] The first one includes antimony-bridged [1]ferrocenophanes of type **II** which feature a bulky aryl group appended to the group 15 center.[12] The stabilization provided by the 2,6-dimesitylphenyl group in **IIb** has allowed for the isolation and characterization of the monomer, which can be subsequently polymerized. Parallel efforts from our group have investigated the less sterically demanding phenyl substituent at antimony.[13] While we were not able to isolate the corresponding [1]ferrocenophane derivative, we succeeded in obtaining respectable yields of the distiba[1.1]ferrocenophanes of type **III**. Keeping in mind that larger oligomers are known in the case of the phosphorus systems,[10] we have now decided to take a more careful look at the product of the reaction leading to **III**.

In this communication, we report that this reaction also affords a trimeric [1.1.1]ferrocenophane and a tetrameric [1.1.1.1] ferrocenophane, the structures of which have been established. As part of our interest toward the development of antimony-based gold(I) systems as catalysts,[14-16] we also describe our efforts to use these antimony macrocycles as ligands for gold(I) cations and as a scaffold for carbophilic reactivity.

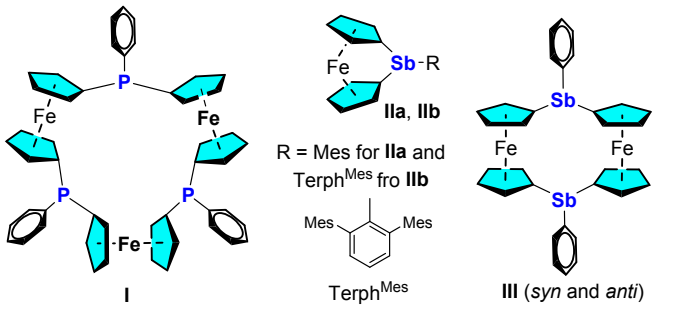

Fig. 1. Selected examples of pnictogen-containing ferrocenophanes.

To begin, a dilute solution of 1,1′-dilithioferrocene·tmeda (tmeda = *N,N,N′,N′*-tetramethylethylenediamine) was treated with one equiv. of $PhSbCl_2$ to afford a mixture of products from which Sb_3 (**1**) and Sb_4 (**2**) macrocycles were prudently isolated as yellow-orange solids in 4% and 3% yield respectively along with compound **III** (6%), following silica gel column chromatography (Fig. 2a). Compounds **1** and **2** provide the first example of macrocyclic Sb_3 and Sb_4 ferrocenophanes. While **1** is the antimony analog of **I**, tetrameric **2** is unprecedented in the chemistry of group 15 ferrocenophanes, even though such structures have been observed in the chemistry of

[a] Department of Chemistry, Texas A&M University, College Station, TX 77843, USA. E-mail: francois@tamu.edu

† Electronic supplementary information (ESI) available: Additional experimental and computational details and crystallographic data in CIF format. CCDC: 2551732-2551734. For ESI and crystallographic data in CIF or other electronic format See DOI: 10.1039/x0xx00000x.

View Article Online
DOI: 10.1039/D6CC02816K

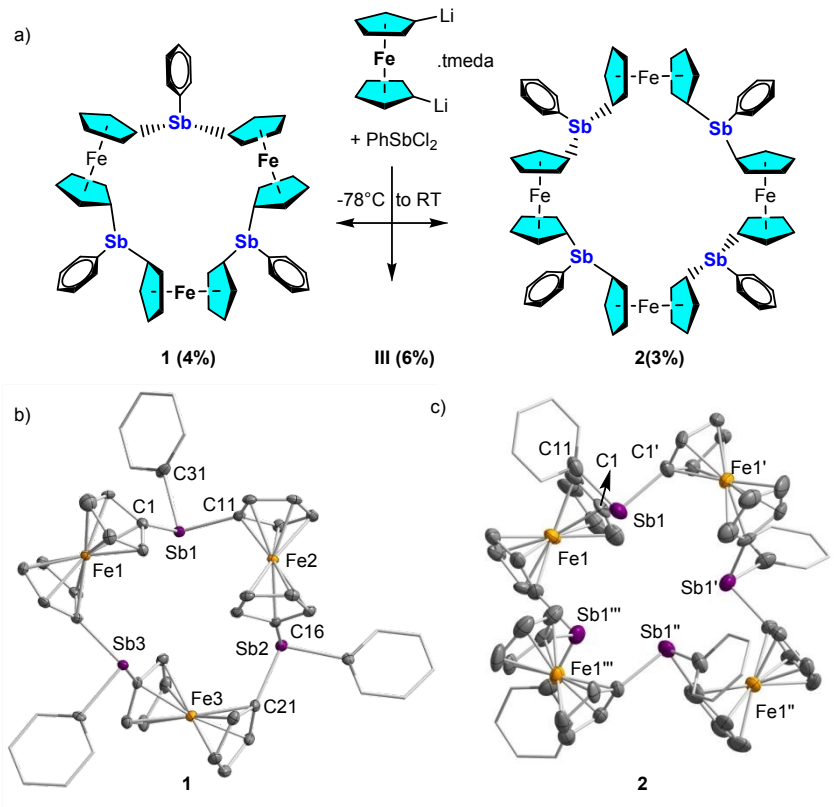

Fig. 2 (a) Synthesis of **1** and **2**. Solid-state structures of (b) **1** and (c) **2**. Thermal ellipsoids are drawn at the 50% probability level. The hydrogen atoms and interstitial solvent molecules are omitted for clarity. Selected atoms are labeled. Selected bond lengths (Å) and angles (°): **1**: Sb1–C1 2.135(4), Sb1–C11 2.123(5), Sb1–C31 2.151(5), Sb2–C16 2.134(5), Sb2–C21 2.133(5); C1-Sb1-C11 97.83(18), C1-Sb1-C31 94.26(18): **2**: Sb1–C1 2.152(10), Sb1–C11 2.160(15); C1-Sb1-C11 95.2(5), C1-Sb1-C1' 93.3(5).

silaferocenophanes.[17] It is notable that **1** and **2** were isolated directly from the reaction mixture at room temperature without light irradiation or heating of their isolated monomer, an approach used for the generation of polyferrocene materials[17, 18] ^{1}H NMR spectroscopy indicates the presence of non-equivalent ferrocene units for both **1** and **2** in solution that are differentiated by their cyclopentadienyl (Cp) proton resonance integration. In the case of **1**, the ^{1}H NMR spectrum can be interpreted based on 12 resonances with four of them accidentally overlapping in pairs. This spectrum indicates that all Cp rings are non-equivalent and that the molecule lacks any symmetry. This spectrum is consistent with the crystal structure of this derivative, which shows a trimeric motif in the asymmetric unit with no apparent symmetry element. The lack of symmetry in the structure of **1** is in contrast to the observed C_3 and C_s symmetry of the phosphorus analog.[10] The lack of symmetry in **1** also manifests in the differing Sb-Sb distances of 4.875(6) Å (Sb1-Sb2), 5.691(6) Å (Sb2-Sb3) and 5.024(6) Å (Sb1-Sb3) as established by single-crystal X-ray diffraction analysis (scXRD) (Fig 2b). A similar situation is encountered in the case **2**, which is best interpreted on the basis of 16 individual resonances, with the accidental overlap of six of them leading to 13 observed massifs. Recording the ^{1}H NMR spectra were recorded for **1** and **2** in $CDCl_3$ at 55 °C does not induce notable spectral changes, highlighting the non-fluxional nature of these macrocycles under these conditions (Fig S12 and S13). In contrast and somewhat surprisingly, **2** crystalizes as a rare S_4 tetramer as shown in Fig. 2c, with a unique Sb-Sb separation of 4.5097(12) Å. The antimony atoms adopt a trigonal pyramidal geometry with the C(Cp)-Sb-C(Cp) angles for **1** in the range of 93.8(2)°- 97.8(2)°, close to the value of 93.3(5)° measured for **2**.[13] The UV-vis spectra of compounds **1** and **2** display weak d–d transitions at λ_{max} = 451 and λ_{max} = 454 nm, respectively, (Fig S17) which is consistent with the spectral features of other ferrocenophanes.[19, 20] The presence of multiple ferrocene units in these systems prompted us to explore their electrochemical behaviour. When scanned anodically at rate of v = 100 mV s^{-1}, the cyclic voltammogram of **1** displays three pseudo reversible oxidation waves at $E^1_{½}$ = 0.045 V, $E^2_{½}$ = 0.195 V, and $E^3_{½}$ = 0.327 V vs $Fc^{+/0}$ (Fig. S18). These features are similar to those of a previously reported trisilaferrocenophane that shows three reversible oxidations.[17] On the other hand, the tetrameric macrocycle **2** exhibits four pseudo reversible oxidation events at $E^1_{½}$ = 0.070 V, $E^2_{½}$ = 0.103 V, $E^3_{½}$ = 0.246 V, and $E^4_{½}$ = 0.286 V vs $Fc^{+/0}$ (Fig S18). This electrochemical behaviour is again reminiscent of an analogous silicon-based ferrocenophane,[17] with two sets of a pair of closely spaced oxidation waves, with the caveat that the associated cathodic waves of each pair of closely spaced peaks appear as a single two-electron reduction event.[17]

We next investigated the ligand behavior of these new systems towards gold(I).[14, 15] Treating **1** with 1 equivalent of AuI in CH_2Cl_2 afforded compound **3** in 73% yield (Fig. 3a). The formation of **3** was confirmed by spectroscopic analysis.

View Article Online
DOI: 10.1039/D6CC02816K

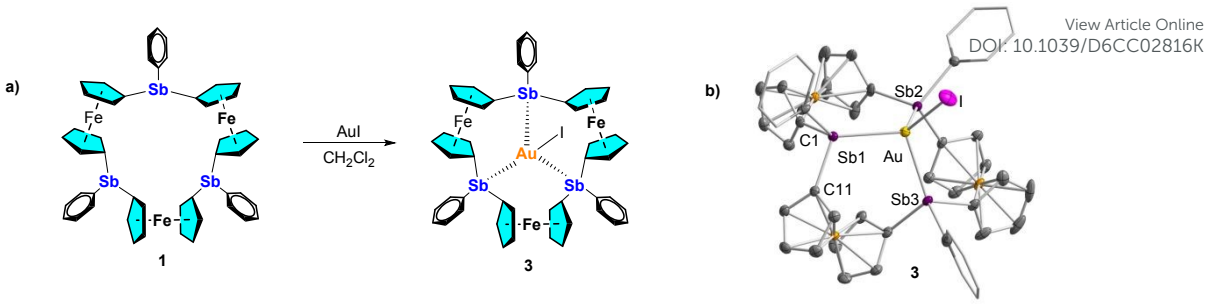

Fig. 3 (a) Synthesis of **3** (b) Solid state structure of **3**. Thermal ellipsoids are drawn at the 50% probability level. The hydrogen atoms and interstitial solvent molecules are omitted for clarity. Selected atoms are labeled. Selected bond lengths (Å) and angles (°): **3**: Sb1–C1 2.121(3), Sb1–C11 2.127(3), Sb1-Au 2.628(3), Sb2-Au 2.611(3), Sb3-Au 2.627(5), Au-I 2.747(9); C1-Sb1-C11 97.9(13), C11-Sb1-Au 117.8(8), Sb1-Au-Sb2 105.5(8), Sb2- Au-Sb3 104.5(3), Sb1-Au-Sb3 102.0(6).

Complexation with gold iodide generates a more symmetrical structure with only three ^{1}H (in the 1:1:2 ratio) and five ^{13}C NMR signals due to the presence of three equivalent ferrocene units. The X-ray crystal structure of **3** is shown in Fig 3b, where the three antimony donors surround the gold center with Au-Sb bond distances of 2.628(3) Å, 2.611(3) Å, and 2.627(5) Å which are comparable with those found in tri-stibine gold complexes.[21] The coordination sphere of the gold center also includes the iodide ligand, bound *via* an Au-I bond of 2.747(9) Å. The tetrahedral coordination geometry of the gold center shows only minor distortions as indicated by the Sb-Au-Sb angles of 105.5(8)°, 104.5(3)°, and 102.0(6)°. We found that **2** also reacted with AuI, as supported by ESI-MS, which showed a peak corresponding to [**2**-Au]$^{+}$ at m/z value of 1728.7263. Unfortunately, attempts to crystallize the corresponding gold complex were unsuccessful. For this reason, additional investigation of this family of compounds focused on **1** and its gold complexes. Intrigued by the possibility of using such macrocyclic antimony ligands as platforms for gold-mediated carbophilic catalysis,[22] we decided to test **3** in the cycloisomerization of the *N*-propargyl-4-fluorobenzamide, **4**, a substrate that we have often used to benchmark the catalytic activity of gold complexes.[23-26] Monitoring by ^{1}H NMR spectroscopy indicated negligible or no conversion to the cyclic product **5** (Supporting Information S19). By contrast, an active catalyst could be generated by the combination of **1** with one equiv. of (tht)AuCl (tht = tetrahydrothiophene) in CH_2Cl_2, as indicated by the rapid conversion of the N-propargyl-4-fluorobenzamide **4** into **5**. The reaction reached a conversion of 94% after 90 minutes (Fig 4, Fig S20). Although we were not able to isolate the gold chloride complex of **1**, which we assume is responsible for the observed activity, its formation is supported by *in situ* ^{1}H NMR spectroscopy (Fig S15) and by ESI-MS, which showed a peak corresponding to [**1**-Au]$^{+}$. For comparative purposes, we also tested the catalytic activity of pure (tht)AuCl and compound **1** alone (Fig. S21, S22). At the same time point and under analogous reaction conditions, the use of (tht)AuCl led to very low conversion (9%), while compound **1** was simply inactive.

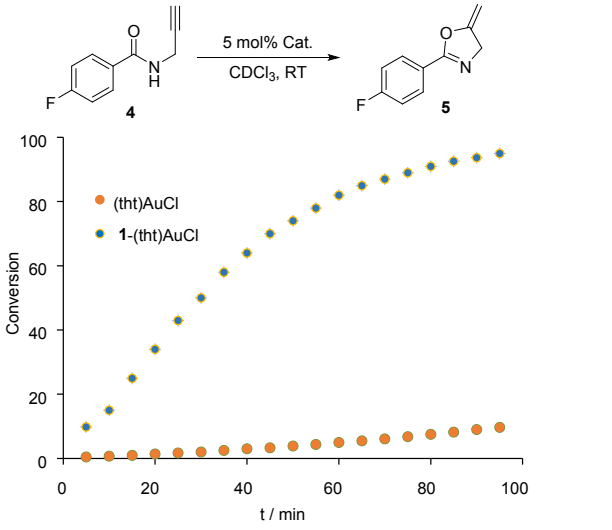

Fig. 4 Cycloisomerization of *N*-propargyl-4-fluorobenzamide, **4** as a function of time in the presence of different catalysts. See figure for conditions.

This work describes heretofore unknown macrocyclic tri- and tetra-stibine featuring 1,1'-ferrocenediyl as linkers. In addition to reporting the isolation and structural characterization of these species, our work shows that these compounds may serve as ligands for gold(I) center, as unambiguously established in the case of the tristibine system. Interestingly, combining the tridentate derivative with a gold(I) chloride precursor forms a catalytically active stibine-gold complex that readily cyclizes propargylic amide in the absence of an added activator. The mechanism by which the catalysis occurs implies dissociation of the chloride ligand, a possibility that we have not yet been able to verify. Ongoing studies aim to shed light on this puzzling aspect.

Author contributions

A.T and S. B. contributed equally to this study. AT has isolated and characterized compounds **1** and **2** and performed the catalytic activity of **1**. S. B. synthesized and characterized compound **3**. M.K finalized the CIF of **1**-**3**. F. P. G. directed the study and corrected the original draft. All co-authors participated in the preparation of the manuscript.

Conflicts of interest

There are no conflicts to declare.

Data availability

The data supporting this article can be found in the supplementary information (SI). Supplementary information: this SI contains synthetic details, characterization data, spectroscopic data, crystallographic details, and computational details. See DOI: https://doi.org/10.1039/d5cc06492a. CCDC: 2551732-2551734 contain the supplementary crystallographic data for this paper.

Acknowledgements

This work was fully carried out at Texas A&M University with support from the Department of Energy (DE-SC0023269) and the Welch Foundation (A-1423).

Notes and references

1. T. Mizuta, Y. Imamura, K. Miyoshi, H. Yorimitsu and K. Oshima, *Organometallics*, 2005, **24**, 990–996.
2. T. Mizuta, Y. Imamura and K. Miyoshi, *J. Am. Chem. Soc.*, 2003, **125**, 2068–2069.
3. E. Khozeimeh Sarbisheh, J. Esteban Flores, J. Zhu and J. Müller, *Chem. Eur. J.*, 2016, **22**, 17048–17048.
4. M. P. T. Cao, J. W. Quail, J. Zhu and J. Müller, *Organometallics*, 2019, **38**, 2092–2104.
5. S. K. Patra, G. R. Whittell, S. Nagiah, C.-L. Ho, W.-Y. Wong and I. Manners, *Chem. Eur. J.*, 2010, **16**, 3240–3250.
6. C. H. Honeyman, T. J. Peckham, J. A. Massey and I. Manners, *Chem. Commun.*, 1996, DOI: 10.1039/CC9960002589, 2589–2590.
7. C. H. Honeyman, D. A. Foucher, F. Y. Dahmen, R. Rulkens, A. J. Lough and I. Manners, *Organometallics*, 1995, **14**, 5503–5512.
8. H. P. Withers, Jr., D. Seyferth, J. D. Fellmann, P. E. Garrou and S. Martin, *Organometallics*, 1982, **1**, 1283–1288.
9. T. Baumgartner and R. Réau, *Chem. Rev.*, 2006, **106**, 4681–4727.
10. T. Mizuta, T. Aotani, Y. Imamura, K. Kubo and K. Miyoshi, *Organometallics*, 2008, **27**, 2457–2463.
11. C. Spang, F. T. Edelmann, M. Noltemeyer and H. W. Roesky, *Chem. Ber.*, 1989, **122**, 1247–1254.
12. H. K. S. Young, H. N. L. Leslie, B. O. Patrick, E. A. LaPierre and I. Manners, *Inorg. Chem.*, 2026, **65**, 2833–2840.
13. A. Thakur, B. L. Murphy, Y. Jiang, N. Bhuvanesh and F. P. Gabbaï, *Chem. Commun.*, 2026, **62**, 5293–5296.
14. J. Schulz, J. Antala, D. Rezazgui, I. Císařová and P. Štěpnička, *Inorg. Chem.*, 2023, **62**, 14028–14043.
15. D. Rezazgui, J. Schulz and P. Štěpnička, *Inorg. Chem.*, 2025, **64**, 11075–11092.
16. N. Seal, D. S. N. D. Samarasinghe, N. Vodnala, M. A. Siegler, C. M. Aikens and A. Das, *Chem. Mater.*, 2025, **37**, 9908–9918.
17. D. E. Herbert, J. B. Gilroy, W. Y. Chan, L. Chabanne, A. Staubitz, A. J. Lough and I. Manners, *J. Am. Chem. Soc.*, 2009, **131**, 14958–14968.
18. A. Berenbaum, H. Braunschweig, R. Dirk, U. Englert, J. C. Green, F. Jäkle, A. J. Lough and I. Manners, *J. Am. Chem. Soc.*, 2000, **122**, 5765–5774.
19. J. Ward, S. Al-Alul, M. W. Forbes, T. E. Burrow and D. A. Foucher, *Organometallics*, 2013, **32**, 2893–2901.
20. R. A. Musgrave, A. D. Russell and I. Manners, *Organometallics*, 2013, **32**, 5654–5667.
21. V. R. Bojan, E. J. Fernández, A. Laguna, J. M. López-de-Luzuriaga, M. Monge, M. E. Olmos, R. C. Puelles and C. Silvestru, *Inorg. Chem.*, 2010, **49**, 5530–5541.
22. J. C. Pérez-Sánchez, R. P. Herrera and M. C. Gimeno, *Eur. J. Inorg. Chem.*, 2022, **2022**, e202101067.
23. B. Zhou, S. Bedajna and F. P. Gabbaï, *Chem. Commun.*, 2024, **60**, 192–195.
24. P. Castro Castro and F. P. Gabbaï, *Organometallics*, 2024, **43**, 2334–2341.
25. S. Sen and F. P. Gabbaï, *Chem. Commun.*, 2017, **53**, 13356–13358.
26. E. D. Litle, L. C. Wilkins and F. P. Gabbaï, *Chem. Sci.*, 2021, **12**, 3929–3936.

View Article Online
DOI: 10.1039/D6CC02816K

Data availability

The data supporting this article can be found in the supplementary information (SI). Supplementary information: this SI contains synthetic details, characterization data, spectroscopic data, crystallographic details, and computational details. See DOI: https://doi.org/10.1039/d5cc06492a. CCDC: 2551732-2551734 contain the supplementary crystallographic data for this paper.